

Monitoring Concepts Using Borehole Transient Electromagnetic and DC Resistivity Methods: 3D Simulation Studies for the Effective Detection of CO₂ Leakages

Jana Börner¹, Martin Afanasjew^{1,2}, Felix Eckhofer², Julia Weißflog¹, and Klaus Spitzer¹
¹Institute of Geophysics and Geoinformatics, ²Institute of Numerical Analysis and Optimization
Technical University Bergakademie Freiberg

SUMMARY

We present a feasibility study for a 3D-time-lapse electromagnetic monitoring concept combining surface direct current (DC) resistivity and borehole transient electromagnetic (BTEM) measurements. The early detection of CO₂ leaking from underground storages into shallow aquifers is a major safety issue. Since electric conductivity is highly sensitive to the presence of CO₂ within water-bearing porous media, geo-electromagnetic methods provide an easy-to-apply, non-invasive and cost-effective way of monitoring large-scale targets.

To understand the petrophysical background, we have developed laboratory equipment to quantify the conductivity change arising from dissolving CO₂. The test conditions represent characteristic p/T-scenarios for depths up to 200m. From the data we derive a petrophysical model to predict the conductivity contrast. Based on this, 3D numerical simulation studies show how to design a well-performing monitoring arrangement. We propose the combination of the DC resistivity and the BTEM method with complementary sensitivity patterns to enhance the subsurface resolution.

Our simulation studies are carried out using state-of-the-art in-house software developed by our working group. The governing partial differential equations are discretized using higher-order Lagrange and Nédélec finite element formulations on unstructured grids giving excellent flexibility with respect to arbitrary model geometry. The time domain problem is particularly demanding. To reduce the numerical effort we have developed Krylov subspace techniques in both the time and frequency domains.

Keywords: forward modeling, finite elements, borehole transient electromagnetics, DC resistivity, CO₂ leakage detection

INTRODUCTION

Monitoring concepts need to resolve particular structures within the subsurface as a function of time. Often the target structures are located at large depths and are of small size. Therefore, the sensitivity pattern of the applied method has to be adopted in such a way that the resolution is focused around the location of the target and its expected temporal change.

As an example, we address the field of CO₂ storage and the early detection of CO₂ leaking from underground storages into shallow aquifers. Reliable and cost-effective monitoring of large subsurface regions to detect CO₂ leakages at an early stage is a challenging task. Uncontrolled migration of CO₂ may harm the environment and poses a safety risk for humans and animals. Electromagnetic methods provide a promising approach to detect CO₂ in the underground because the electrical conductivity is highly sensitive to the presence of CO₂ (Börner, Herdegen, Repke, & Spitzer, 2012). To enhance the resolution at depth we use a borehole-based transient electromagnetic technique (BTEM). In addition, we combine BTEM with surface DC resistivity measurements to cover

a wide spatial range reaching up to the surface.

In order to obtain robust and high-quality monitoring results we have to merge different fields from mathematics, geophysics and geoinformatics in an interdisciplinary way (Fig. 1).

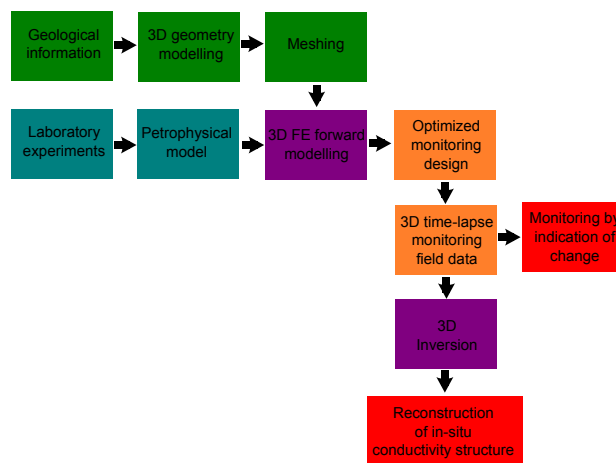


Figure 1. Workflow for reliable and robust electromagnetic monitoring.

Techniques from geoinformatics and 3D geographic information systems govern and visualize realistic 3D geometries (Fig. 2). Laboratory experiments provide the data base and the knowledge of petrophysical processes within the reservoir and the link with the electric properties of a complex composite material such as rock. Numerical techniques allow for the realistic simulation of electromagnetic fields in complicatedly structured three-dimensional media. Discretizing the modeling domain using vector finite elements on unstructured grids facilitates the flexible incorporation of complex internal structures and/or surface topography. The simulation results may, in return, serve to optimize the monitoring design, which finally leads to high-quality sensitive field data.

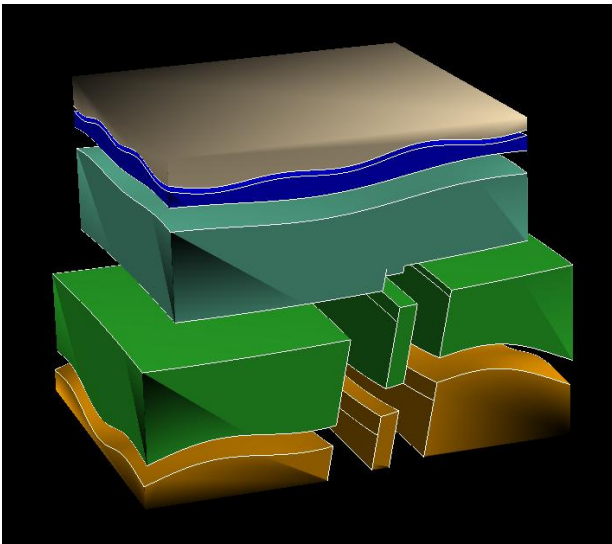
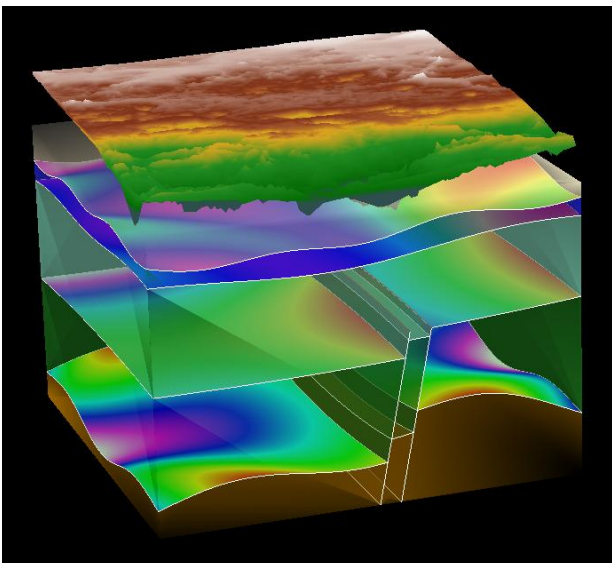


Figure 2. Geologic scenario for CO₂ leakage modeled with Gocad[®]. Top: geologic assembly, bottom: conductivity domains. The slanted, sub-vertical structure represents a fracture zone.

3D data sets may be used both for time-lapse monitoring by comparing the data of succeeding measurements and as an input for enhanced inversion schemes in order to reconstruct the conductivity distribution within the earth.

PETROPHYSICAL SETTING

The impact of CO₂ on the electrical conductivity is due to two major mechanisms:

- Resistive CO₂ displaces conductive pore fluid thus decreasing the rock conductivity.
- CO₂ dissolves in the pore water until thermodynamical equilibrium is reached thereby increasing the conductivity by providing additional charges.

The evolution of a free CO₂ phase is mainly expected within the storage reservoir, whereas small but continuous amounts of CO₂ leaking into shallow and electrically resistive aquifer systems cause conductive anomalies due to the dissolution processes.

The data we acquired in laboratory experiments suggest an adapted formulation of Archie's law accounting for the change in pore water conductivity as a function of pressure (Börner *et al.*, 2012):

$$\sigma_{el} + \sigma_{dis} = \Phi^m S_w^n \sigma_w \left(1 + t_s \left(1 - e^{-c_p(p/p^o)} \right) \right), \quad (1)$$

where $\sigma_{el} + \sigma_{dis}$ is the total electrolytic conductivity including the part from CO₂ dissociation, σ_w the pore water conductivity, Φ the porosity, S_w the saturation, t_s a saturation threshold, c_p a pressure coefficient, p^o a reference pressure, and m and n Archie's empirical parameters depending on the rock formation characteristics.

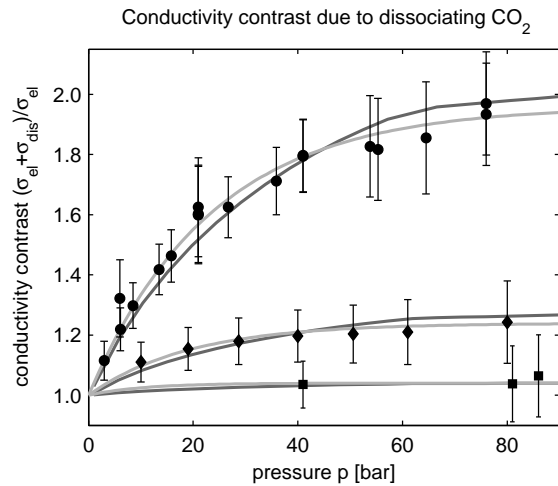


Figure 3. Increase of water conductivity with CO₂ pressure p at temperature $T = 25^\circ\text{C}$ for low-saline fluid (dots), moderately saline fluid (diamonds), and highly saline fluid (squares) (from (Börner *et al.*, 2012)).

This model allows the prediction of conductivity contrasts for known rock formations. Fig.3 shows the water conductivity as a function of pressure for three different salinities. The light gray lines represent fitted exponential curves according to the dissociation term in equation (1) and the dark gray curves represent geochemical modeling results. The impact of dissolving CO₂ on water conductivity is largest for the lowest salinity.

3D DC RESISTIVITY MODELING USING THE SECONDARY FIELD APPROACH

All DC resistivity modeling results presented in the following are produced by the secondary potential finite element code of Weißflog *et al.* (2012). Modeling DC resistivity requires the discretization of the equation of continuity:

$$-\nabla \cdot (\sigma \nabla V) = I \delta(\mathbf{x} - \mathbf{x}_0) \quad (2)$$

with V as the electric potential, conductivity σ and a point source of strength I located at \mathbf{x}_0 . The source term introduces a singularity in the potential response, which significantly decreases the convergence rate of the finite element approximation. To avoid this, a secondary field formulation is used. The decomposition of the total potential V into primary (V_p) and secondary potential (V_s) yields the following equation:

$$\begin{aligned} -\nabla \cdot (\sigma \nabla V_s) &= \nabla \cdot (\sigma_s \nabla V_p) \\ &= \nabla \cdot (\sigma \nabla V_p) - \nabla \cdot (\sigma_0 \nabla V_p) \end{aligned} \quad (3)$$

with an anomalous conductivity $\sigma_s = \sigma - \sigma_0$. The discrete representation of equation (3) reads

$$A(\sigma) \mathbf{u}_s = -A(\sigma) \mathbf{u}_p + \sigma_0 A(1) \mathbf{u}_p \quad (4)$$

where A is the system matrix, the vectors \mathbf{u}_p and \mathbf{u}_s contain the total and secondary potentials V , respectively, and, in addition to $A(\sigma)$, only the matrix $A(1)$ has to be assembled. For multiple sources there is no need to re-assemble any matrix. The primary potential may be determined by Green's function. Note that for arbitrary surface topography Green's function still holds if the boundary condition for the secondary field is formulated accordingly. The costly numerical calculation of the total potential for arbitrary surfaces (as described by Rücker, Günther, and Spitzer (2006)) is therefore obsolete, which reduces the amount of numerical work significantly.

The efficiency of the secondary field approach for regular grid refinements is shown by Weißflog *et al.* (2012) in terms of an improved convergence rate.

3D MODELING OF TRANSIENT ELECTROMAGNETIC FIELDS USING KRYLOV SUBSPACE METHODS

In order to carry out the modeling of transient electromagnetic fields in three dimensions we have applied the finite element code of Afanasjew *et al.* (2010), which incorporates rational Krylov subspace methods. The curl-curl equation underlying diffusive electromagnetic induction phenomena reads

$$-\frac{\partial \mathbf{j}_e}{\partial t} = \frac{\partial(\sigma \mathbf{E})}{\partial t} + \nabla \times (\mu^{-1} \nabla \times \mathbf{E}) \quad (5)$$

with \mathbf{E} as the time varying electric field, μ as the magnetic permeability, and \mathbf{j}_e as an imprinted source current density. For simplicity, we choose perfect conductor boundary conditions resulting in a vanishing tangential component of the electric field $\mathbf{n} \times \mathbf{E} = \mathbf{0}$ at all boundaries except for the earth's surface, where an exact boundary condition has been implemented.

The latter is derived from the electric field obeying Laplace's equation in the isolating ($\sigma = 0$) air halfspace (Afanasjew *et al.*, 2010; Goldman, Hubans, Nicoletis, & Spitz, 1986). The semi-discretized formulation of the curl-curl equation (5) thus reads

$$-\frac{\partial \mathbf{E}}{\partial t} = A \mathbf{E} \quad (6)$$

which represents an initial value problem for $\mathbf{E}(t)$ with the initial condition $\mathbf{E}(t_0) = \mathbf{E}_0$ at a time t_0 shortly after the current shut-off. The matrix A is the discrete representation of the curl-curl operator using vector finite elements of the Nédélec type. Eq. (6) is an ordinary differential equation, which has the solution $\mathbf{E}(t) = \exp(A t)$ with \exp as the matrix exponential function.

The direct numerical evaluation of the matrix function is not feasible due to the large size of A . Therefore, the large n -dimensional matrix A is projected onto an m -dimensional Krylov subspace with $m \ll n$. After evaluating the exponential matrix function for the small projected matrix, an approximation of the electric field in the original space may be obtained. Using this method it is possible to approximate the electric field at any given time with only one step allowing for an efficient sampling of any electromagnetic transient.

MODELING RESULTS

First simulations demonstrate the impact of a conductive intrusion of CO₂ rich water into a clean aquifer. Figure 4 shows the undisturbed system (top panel), where the current system mainly concentrates within the aquifer. When CO₂ migrates up the fracture within a small band (center panel) the current is 'caught' by the increased conductivity. At the bottom part of Figure 4 the CO₂ leaks into the aquifer and forms a contamination plume. The current

system then concentrates within the disturbed part of the aquifer, even though the contaminated fracture still may be distinguished from the clean regions.

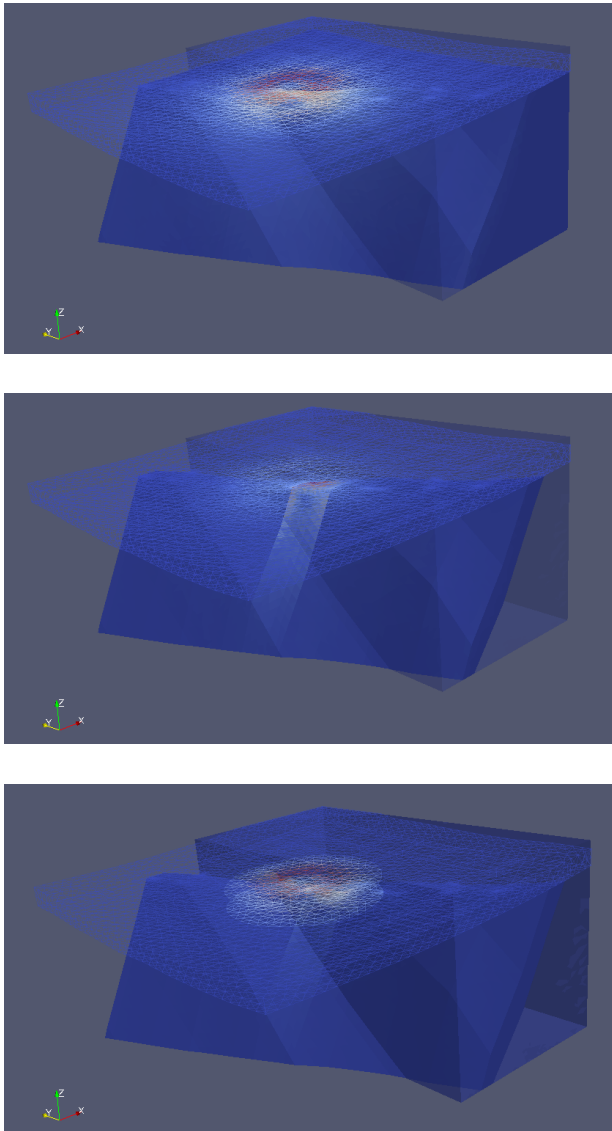


Figure 4. Normalized magnitude of the current density after 4e-5s for a clean aquifer embedded in less-conductive rocks (top), highly conductive CO₂ contamination rising within the fracture zone (center) and CO₂ contamination leaking into the aquifer and forming a plume (bottom).

CONCLUSIONS

We present a model study that illuminates feasible approaches to monitoring large areas with respect to CO₂ leakages. We use a combination of the DC resistivity and BTEM methods. To deal with the complicated natural structures we have developed a number of Lagrange and Nédélec finite element codes in 3D. First modeling results demonstrate the impact of CO₂ on the diffusion of electromagnetic fields. Further studies will focus on the DC

resistivity response. We continue by quantifying the local effect of CO₂ as being monitored from the earth's surface and from within a borehole. The BTEM and DC resistivity equipment is available at the Institute of Geophysics and Geoinformatics of the TU Bergakademie Freiberg so that the concept aims at being transferred into a practical technique.

ACKNOWLEDGMENTS

The authors acknowledge the funding of the laboratory work by the German Research Foundation DFG (grant number SP 356/12-1). The development of the numerical codes were largely supported by the Geotechnologien Program of the German Ministry of Education and Research BMBF and the DFG (grant number 03G0746B).

REFERENCES

- Afanasjew, M., Börner, R.-U., Eiermann, M., Ernst, O., Güttel, S., & Spitzer, K. (2010). Two-dimensional time domain TEM simulation using finite elements, an exact boundary condition, and krylov subspace methods. In *20th IAGA International Workshop on Electromagnetic Induction in the Earth, Expanded Abstracts*, 4 p.
- Börner, J. H., Herdegen, V., Repke, J.-U., & Spitzer, K. (2012). The impact of CO₂ on the electrical properties of water bearing porous media - laboratory experiments with respect to carbon capture and storage. *Geophysical Prospecting*, DOI: 10.1111/j.1365-2478.2012.01129.x, 15 p.
- Goldman, Y., Hubans, C., Nicoletis, S., & Spitz, S. (1986). A finite-element solution for the transient electromagnetic response of an arbitrary two-dimensional resistivity distribution. *Geophysics*, 51, 1450-1461.
- Rücker, C., Günther, T., & Spitzer, K. (2006). 3-d modeling and inversion of DC resistivity data incorporating topography - part I: Modeling. *Geophys. J. Int.*, 166, 495-505.
- Weißflog, J., Eckhofer, F., Börner, R.-U., Eiermann, M., Ernst, O., & Spitzer, K. (2012). 3D DC resistivity FE modelling and inversion in view of a parallelised Multi-EM inversion approach. In *21st IAGA International Workshop on Electromagnetic Induction in the Earth, Expanded Abstracts*, 4 p.